

“BURSTY” RECONNECTION FOLLOWING SOLAR ERUPTIONS: MHD SIMULATIONS AND COMPARISON WITH OBSERVATIONS

PETE RILEY, ROBERTO LIONELLO, ZORAN MIKIĆ, JON LINKER, AND ERIC CLARK
Science Applications International Corporation, San Diego, CA; pete.riley@saic.com, lionelr@saic.com,
mikicz@saic.com, linkerj@saic.com, stephen.e.clark@saic.com

AND

JUN LIN AND YUAN-KUEN KO
Harvard-Smithsonian Center for Astrophysics, Cambridge, MA; jlin@cfa.harvard.edu, yko@cfa.harvard.edu
Received 2006 July 12; accepted 2006 October 3

ABSTRACT

Posteruptive arcades are frequently seen in the aftermath of coronal mass ejections (CMEs). The formation of these loops at successively higher altitudes, coupled with the classic “two-ribbon” flare seen in $H\alpha$, are interpreted as reconnection of the coronal magnetic field that has been dragged outward by the CME. White-light observations of “rays,” which have been interpreted as being coincident with the current sheet at the reconnection site underneath the erupting CME, also provide evidence for its occurrence. “Blobs” occasionally seen within these rays suggest an even richer level of structure. In this report, we present numerical simulations that reproduce both the observed rays and the formation and evolution of the blobs. We compare their properties with *SOHO/LASCO* observations of similar structures, and relate their formation to standard theories of reconnection.

Subject headings: Sun: activity — Sun: corona — Sun: coronal mass ejections (CMEs) —
Sun: magnetic fields — solar wind

Online material: color figures, mpeg animations

1. INTRODUCTION

Since coronal mass ejections (CMEs) were first discovered in the early 1970s, many of their properties have been catalogued, and progress has been made in understanding the processes related to initiation and propagation. While the basic pre-eruption configuration and the topological changes in the magnetic field that result in the conversion of magnetic energy into the kinetic energy of the eruption are not well understood, a standard picture of the posteruption aftermath of CMEs has emerged (Forbes 2000).

Observations by the *LASCO* instrument on board *SOHO* have revealed a wealth of information related to the evolutionary properties of coronal mass ejections (CMEs) close to the Sun. In particular, Wang et al. (1999) reported on small, faint inflows at distances of $2\text{--}4 R_{\odot}$. These cusplike features moved toward the Sun with speeds ranging from 20 to 100 km s⁻¹. Since they tended to occur ~ 1 day following the passage of a CME, they were interpreted as signatures of the closing down of magnetic flux expelled by the CME. During the late stages of an eruption, as the flux rope is propagating away from the Sun, bright “rays” are occasionally observed, which connect the growing hot loop arcade with the trailing portion of the ejecta (Ko et al. 2003; Webb et al. 2003; Lin et al. 2005). In some cases, “blobs” are seen within the rays (Ko et al. 2003; Lin et al. 2005). Observations by *SOHO/EIT* have also demonstrated the basic physical properties of: (1) posteruptive arcades (Tripathi et al. 2004); and (2) coronal downflow related to a prominence eruption associated with a CME (Tripathi et al. 2006). Finally, structure inferred from soft X-ray observations by the *Yohkoh* spacecraft has been interpreted as the signature of the re-formation of the helmet streamer (Hiei et al. 1993), and even direct evidence of high-speed flows above the reforming loops (McKenzie & Hudson 1999, 2001).

We have used numerical simulations to interpret solar and in situ observations associated with the posteruption reconnection site beneath the CME. Riley et al. (2002) identified a signature of the reconnection process in the form of a velocity enhancement that trailed the flux rope all the way out to 1 AU. We found several examples of magnetic clouds with precisely these signatures, suggesting that at least some of these signatures might be associated with jetted outflow in the reconnection region and not with prominence material, as had been previously suggested. Webb et al. (2003) investigated the properties of current sheets trailing CMEs (as inferred from white-light observations of these rays), and compared them with analytical (Lin & Forbes 2000) and numerical (Linker et al. 2003a) models. Webb et al. found that the simulations reproduced the essential characteristics of the rays (e.g., duration and extent).

The aim of this brief report is to: (1) present numerical simulations that reproduce the formation and evolution of blobs; and (2) compare these results with *SOHO/LASCO* observations of blobs. In the next section, we summarize an event observed by the *LASCO* instrument on board *SOHO*. Following that, we describe numerical simulation results that show the formation and propagation of blobs. Finally, we show that the properties of the reconnection site, as inferred from both observations and simulation results, match standard reconnection theory, and in particular the tearing-mode instability.

2. SOLAR OBSERVATIONS

Figure 1 summarizes the aftermath of an eruption that occurred on 2003 November 18. The event has been described in detail by Lin et al. (2005). The sequence contains a raylike feature bridging the ejecta to the lower corona, together with a sequence of blobs that move along or through the ray. The motion of the blobs is

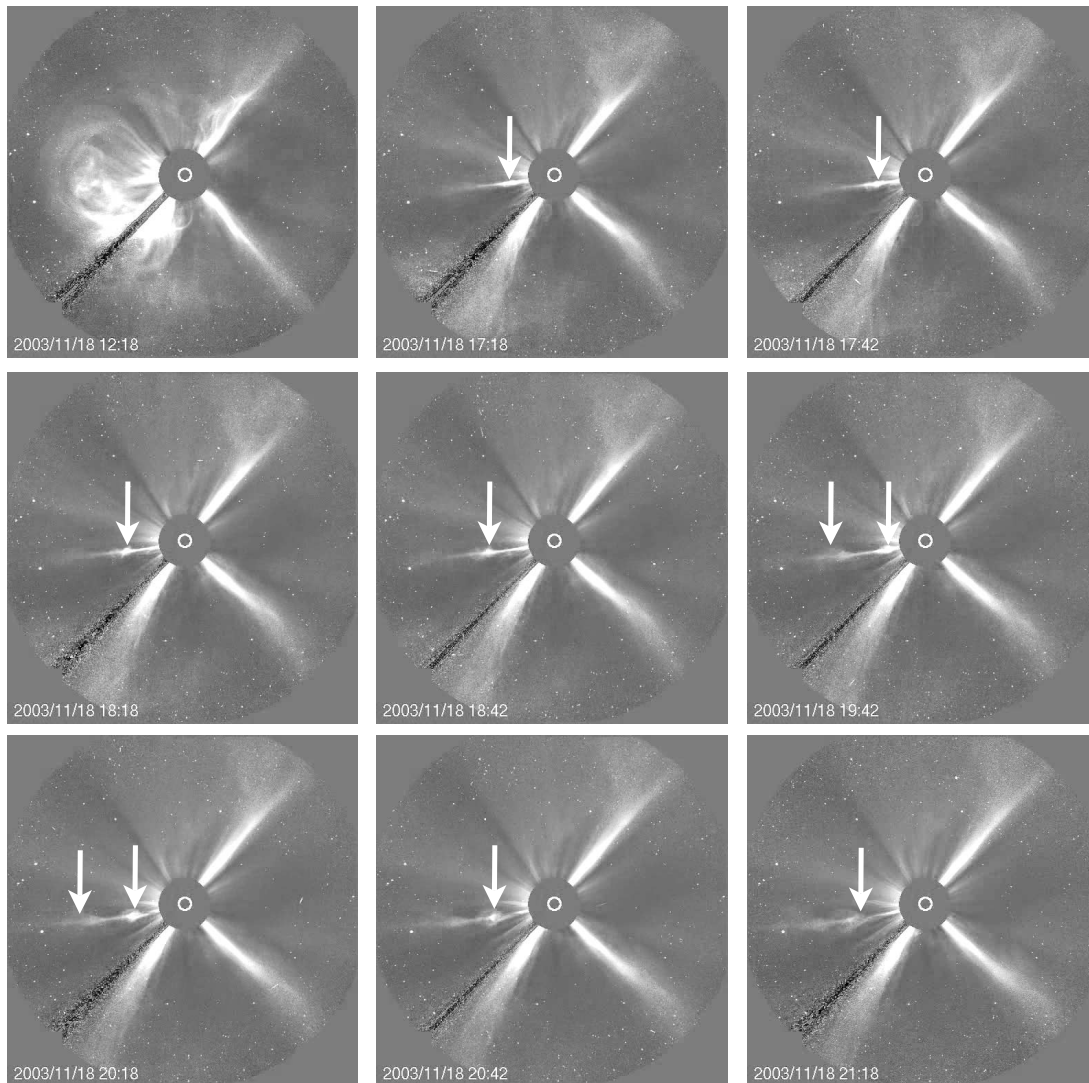


FIG. 1.— Sequence of LASCO/SOHO C3 images during 2003 November 18, summarizing the posteruption structure beneath the CME. The top left panel shows the CME traversing the field of view, while the remaining panels show a bright raylike feature bridging the ejecta to the lower corona, together with a sequence of “blobs” that move along the ray. The position of the blobs are indicated by the vertical white arrows. Note that the first two panels are separated by 5 hr, while the remaining panels are separated by ~ 30 minutes. [See the electronic edition of the *Journal* for a color version of this figure and mpeg animations from the C2 and C3 coronagraphs.]

much more apparent as a movie, which can be viewed in the electronic edition of this article.

Time-height profiles for these blobs are shown in Figure 2. The best-fit lines through these points suggest that blob 1 moves through the field of view with constant speed, while blobs 2–4 are accelerating as they move away from the Sun. A least-squares linear fit to blob 1 yields a speed of 887 km s^{-1} . Results from Lin et al. (2005) indicate that this velocity ranges from 450 to 1000 km s^{-1} .

3. NUMERICAL SIMULATIONS

Our model solves the usual set of time-dependent MHD equations that describe many aspects of the large-scale behavior of the solar corona and inner heliosphere. For this study, we limit our domain from 1 to $30 R_{\odot}$. The details of the algorithm used to advance the equations of the SAIC coronal model are given elsewhere (Mikić & Linker 1994; Lionello et al. 1998; Mikić et al. 1999). The 2.5-dimensional solutions presented here were solved on a nonuniform, spherical (r, θ) grid with Δr ranging from 0.0024 to $0.14 R_{\odot}$ and $\Delta \theta$ ranging from 0.0021 to 0.020 rad. A uniform

resistivity η was used, corresponding to a resistive diffusion time $\tau_R = 4 \times 10^4 \text{ hr}$ (for a length scale of R_{\odot}). At the base of the modeling region (within the helmet streamer), the Alfvén speed (V_{A_0}) was $\sim 967 \text{ km s}^{-1}$, and the Alfvén travel time (τ_A) was 12 minutes. Thus the Lundquist number, $\tau_R/\tau_A \sim 2 \times 10^5$. A uniform viscosity ν was also used, corresponding to a viscous diffusion time $\tau_\nu = R_S^2/\nu$, such that $\tau_\nu/\tau_A = 200$.

Most theories of CME initiation start from the premise that they are triggered by the release of energy stored in the coronal magnetic field (e.g., Forbes 2000). In some theories, reconnection prior to eruption is crucial for initiating the CME (e.g., the “breakout” model [Antiochos et al. 1999]), while in others, it may be incidental (Török & Kliem 2005). Regardless of whether reconnection plays a role in initiating the CME, numerical simulations of CMEs should reproduce the posteruption arcades that occur in the standard model (Linker et al. 2003a, 2003b). Such arcades are in fact found in simulations of CME initiation by both shearing flows (Linker & Mikić 1995) and flux cancellation (Linker et al. 2003a), and are part of the process that ejects a magnetic flux rope into the solar wind.

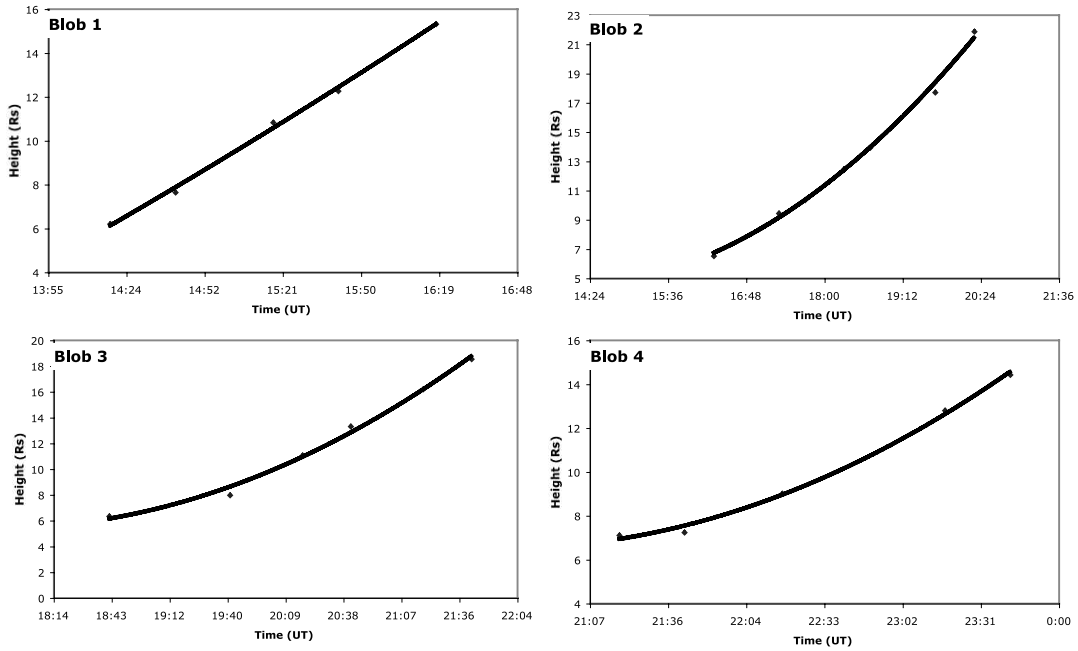


FIG. 2.—Time-height profiles of the 4 blobs shown in Fig. 1. The points indicate the instantaneous position of the blobs as inferred from individual frames, and the solid lines represent least-squares fits to second-order polynomials.

The eruption and early evolution of the flux rope has been described by Riley et al. (2002, 2003). Of particular relevance to this study are the origins of the magnetic field lines that make up the flux rope. These lie in the closed magnetic field embedded within the streamer belt. As the flux rope erupts into the solar corona, overlying field lines, which are still connected back to the Sun at both ends, are brought together under the flux rope. As they reconnect with each other, they contribute both to the flux of the evolving flux rope to the antisunward side of the reconnection site and to the regrowth of the streamer belt on the sunward side.

Figure 3 summarizes the evolution of the current sheet beneath an erupting flux rope. The blue images show simulated polarized brightness, and the contours are the magnetic flux function, equivalent to magnetic field lines in two dimensions. A movie is also available in the electronic version of this article. The panels, which are equally spaced in time ($\Delta t = 30$ minutes), show the repeated formation of a set of blobs that move both toward and away from the Sun. The blobs moving away from the Sun decrease rapidly with intensity (consistent with the observations) as they propagate into a spherically expanding medium. For a similar reason, the blobs moving toward the Sun increase in intensity. We emphasize that this simulation was not specifically constructed to model the 2003 November 18 event. In fact, similar simulations have been used to interpret a number of other events (Riley et al. 2002, 2003). Nevertheless, there is a good general agreement in the formation of a bright ray under the erupting flux rope and the formation and propagation of the blobs away from the Sun. Finally, note that the blobs coincide with *O*-type points in the magnetic field and with *X*-type points lying between them.

In Figure 4 we have computed the time-height profiles for five outwardly-propagating blobs, which showed typical average speeds of $\sim 350 \text{ km s}^{-1}$ and very modest acceleration. In Figure 5 we have repeated this exercise for five inwardly-propagating blobs. Again, all blobs display a small amount of acceleration, and are moving toward the Sun at speeds of $\sim 200 \text{ km s}^{-1}$.

The inflow Mach number (M_A) provides a convenient measure of the reconnection rate. It is defined by

$$M_A = V_i / V_{Ai}, \quad (1)$$

where V_i is the inflow speed into the current sheet and V_{Ai} is the inflow Alfvén speed.

Figure 6 displays the Alfvén Mach number computed for $t = 42$ minutes after the first frame in Figure 3, i.e., between frames 2 and 3. The current sheet is inferred to be the thin red structure located at $1.5 R_\odot \gtrsim x \lesssim 4 R_\odot$ and $y \sim -0.5 R_\odot$. From this we deduce that $M_A = 0.25$. (This is larger than the value ~ 0.1 inferred from a lower resolution simulation using more heuristic means; Webb et al. 2003). Note also that the location of blobs can be inferred from the magnetic field lines, which show *O*-type points within the red region at $x = 2.3 R_\odot$ and $x = 3.6 R_\odot$.

4. SUMMARY AND DISCUSSION

In this report, we have presented results from numerical simulation that reproduce “blobs,” a relatively rare feature of bright rays, which are associated with the reconnection site beneath erupting CMEs. We have computed several basic properties of both the observed and simulated blobs. In particular, the blobs typically display an accelerating speed profile. While there are quantitative differences between the model results and the observations, overall the comparison is relatively good, suggesting that global, resistive MHD models can be used to explore the underlying physical processes at work. A more detailed description of these processes within the context of reconnection theory will form the basis of a future publication. Here we present a more heuristic interpretation of the results.

Standard reconnection theory suggests that the outflow speed (and hence the speed of the blobs) in a frame of reference moving with the solar wind, V_o , is

$$V_o = V_{Ai}(n_i/n_o), \quad (2)$$

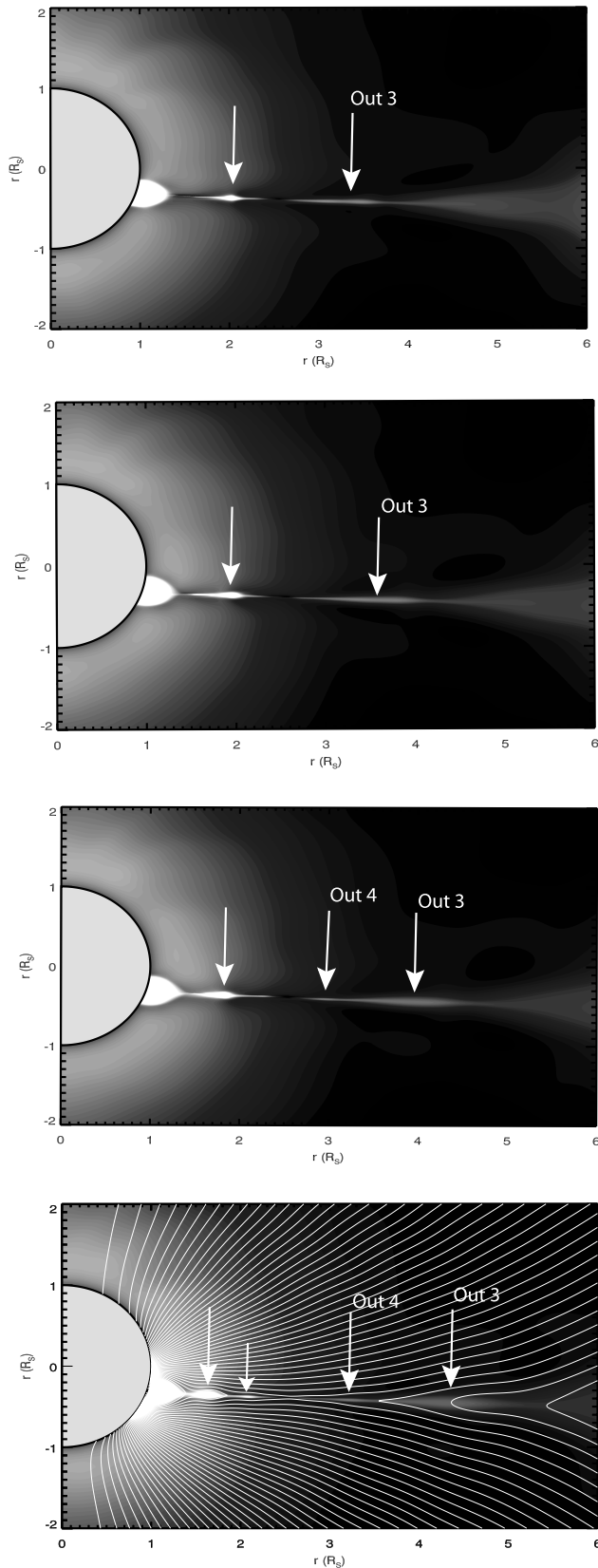


FIG. 3.—Sequence of white-light images from an axisymmetric simulation of a CME eruption based on flux cancellation. White arrows mark the position of both inwardly-propagating and outwardly-propagating blobs in each frame (those at, or below $2 R_{\odot}$ are moving inwards). The two blobs labeled “out 3” and “out 4” correspond to blobs analyzed in Fig. 4. In the bottom frame, the white contours show the magnetic flux function, which in 2.5 dimensions are projections of magnetic field lines. [See the electronic edition of the *Journal* for a color version and *mpeg animation of this figure*.]

where n_i and n_o are the inflow and outflow number densities, respectively. Lin et al. (2005) used (1) LASCO observations of the blobs to infer V_{Ai} ; and (2) UVCS observations to infer V_i . From this, and assuming incompressibility, they deduced M_A to be at in the range of 0.01–0.23. Our compressive MHD simulations, which allow us to compute M_A directly, suggest that $M_A \sim 0.25$ in the vicinity of the current sheet, roughly consistent with the results of Lin et al. (2005). It is also worth noting that the blobs typically show an accelerating profile in both model results and observations. What causes this acceleration? One possibility is that, after being produced, the blobs are “picked up” by the ambient solar wind and accelerated with it. However, the inferred speeds of the blobs computed here and by Lin et al. (2005) are typically much larger than the ambient solar wind speed at these radii. Thus, it is more likely that the ambient wind would act to slow them down. A more likely explanation is that the reconnection process itself accelerates the blobs. Provided no X -type point exists further along the current sheet, the magnetic tension in the field lines recently reconnected will act as a “slingshot,” pulling the blobs away from the Sun.

Neither the observations nor the axisymmetric numerical model results give us an unambiguous picture of the three-dimensional structure of these blobs. In particular, are they cylindrical, with a long axis perpendicular to the observers line of sight, or are they spherical, with an azimuthal extent comparable to either their radial, or meridional extent? The fact that these blobs are not observed very often may tell us something about their geometry. Either they are a rare phenomena or a unique orientation is required for them to be viewed (see also the discussion by Ko et al. 2003). However, rays, while also relatively rare, are observed more frequently without embedded blobs. Thus, it would appear that orientation is already factored into the observations of the rays. That is, it is likely that the observer must view a two-dimensional current sheet end-on. That all rays do not contain blobs further suggests that either the phenomena responsible for the formation of the blobs is not operating all the time, or that the blobs are formed but are not detectable by our instrumentation.

The formation and evolution of the O - and X -type neutral points described here are strongly suggestive of the tearing-mode instability, first described by Furth et al. (1963). They found that a simple, static current sheet would spontaneously reconnect to form a set of magnetic islands, provided that the length of the sheet, l :

$$l > d/(2\pi), \quad (3)$$

where d is the width of the sheet. Based on the white-light images (Figs. 1 and 3), it would appear that this criterion is easily met. The geometry of the current sheet associated with the erupting CME, however, is significantly more complicated than the configuration analyzed by Furth et al. (1963). Bulanov et al. (1978) demonstrated that flow along a current sheet can provide additional stability against the tearing mode. Thus, ambient solar wind flow along either side of the reconnection site may impact the condition for instability. We should note that gravitational and rippling modes can also occur when the density or resistivity varies along the current sheet (Priest & Forbes 2000). These are, however, much smaller scale features than the structures we are describing here.

The tearing-mode instability is not the only theory for time-dependent reconnection. Dungey (1953) described a process known as “ X -type” collapse well before Sweet (1958) or Furth et al. (1963). In addition, Semenov et al. (1983) extended Petschek-type reconnection to include the temporal effects that occur due to an enhanced resistivity at some point in the current sheet.

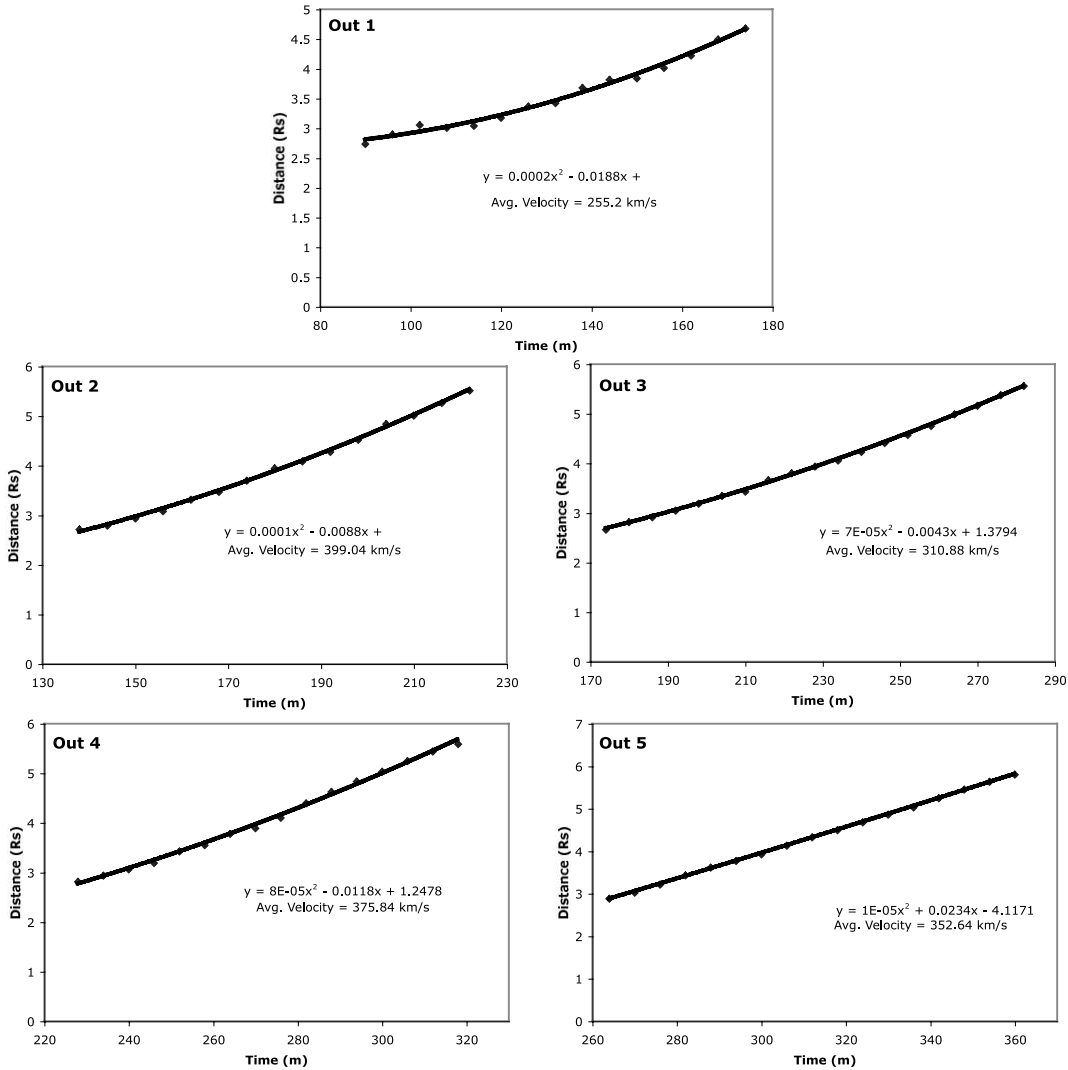


FIG. 4.—Time-height profiles for five outwardly propagating blobs from the simulation, two of which are captured in Fig. 3. The points were computed by tracking the blobs from frame to frame. The solid lines represent least-squares fits to second-order polynomials, the results of which are also shown in each panel.

Given the complexity of the present geometry, it is difficult to relate these idealized theoretical results much beyond the heuristic comments we have made so far. A more productive path, however, would be to use these theories to predict what observational signatures we might look for. All theories would predict strong currents at the X -type points, which might translate into anomalously high temperatures. These temperature peaks would fall between the blobs, which correspond with the O -type points.

It is important to note that while the comparisons between observations and simulations are quite good, they cannot, at this point, be used to prove a direct cause for the observed phenomena. That is, it is possible that some other physical process is at work that is not incorporated into the model. We have not, however, been able to conceive of any alternative theories, and thus we suggest that the tearing-mode instability is the most likely explanation for the observed phenomena.

The simulation presented here is highly idealized for a number of reasons.

1. The geometry is axisymmetric, and thus the erupting CME is really an erupting torus.

2. While the spatial resolution in the meridional plane near the current sheet is relatively high ($\Delta r_{\min} = 0.0024 R_{\odot}$ and $\Delta \theta_{\min} = 0.0021$ rad), it may not capture all of the structure at the reconnection site.

3. The process of reconnection may not be well described within the approximation of resistive MHD.

4. The mechanism used to initiate the CME may not correspond to the actual trigger for the November 18 event.

5. The ambient solar corona prior to the eruption was likely quite different than the idealized conditions used in the model.

The qualitative similarities, however, between the observations and the simulation results suggest that these approximations are justifiable. Note that our preliminary calculations were made at half the resolution of the simulations described here. In those cases, we were not able to resolve any inwardly propagating blobs. Moreover, the outwardly propagating blobs (1) were larger, (2) formed at different times during the simulation, and (3) traveled at different (but comparable) speeds.

Thus, we caution that while our results can be defended qualitatively, it would be premature to conclude that we have captured

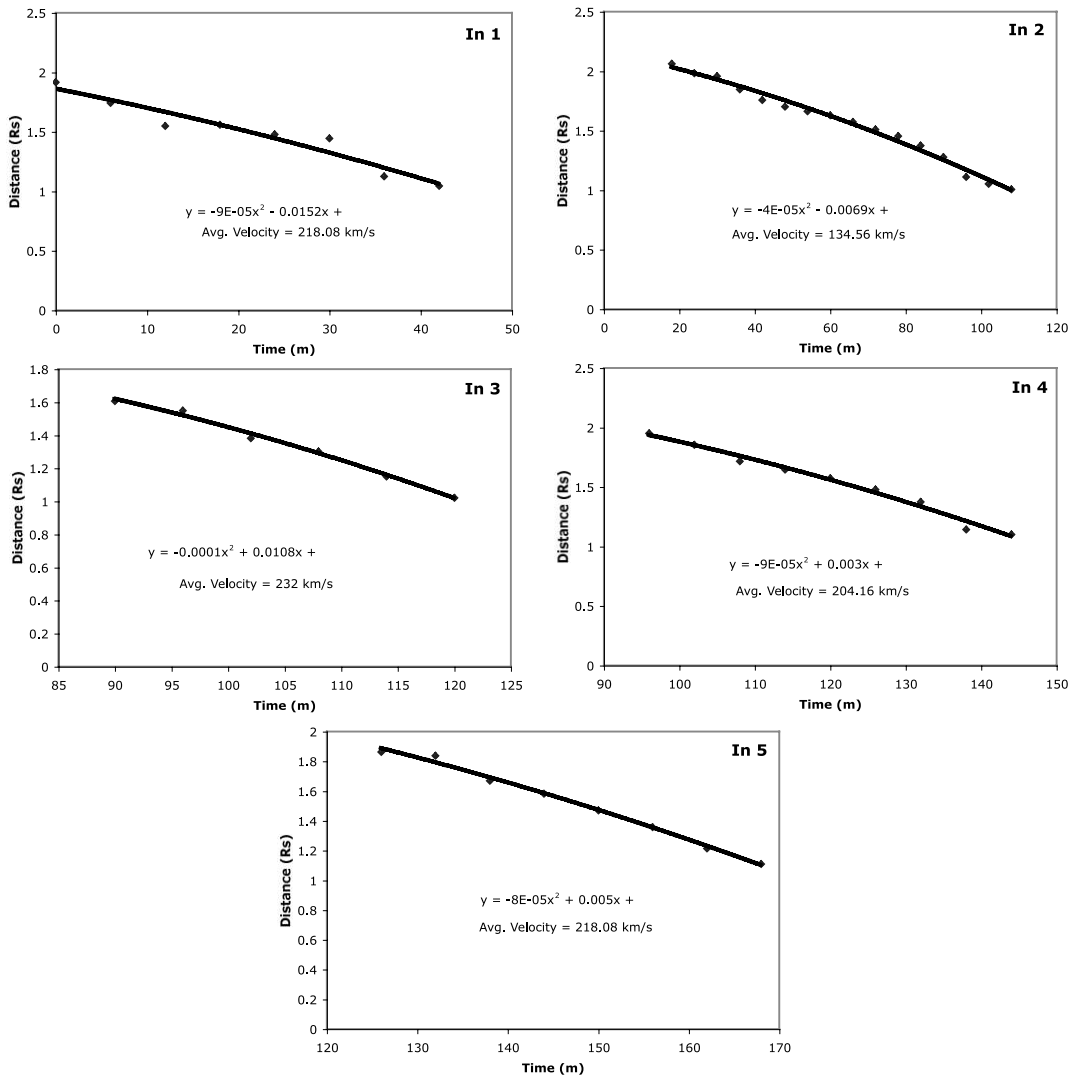


FIG. 5.—As Fig. 3, but for five inwardly propagating blobs.

the quantitative aspects of the evolution of the blobs. The disparity between the observed blob speeds ($\sim 800 \text{ km s}^{-1}$) and the simulated blob speeds ($\sim 350 \text{ km s}^{-1}$), for example, may be a consequence of spatial resolution. Demonstrating convergence at even higher resolution is necessary to defend any quantitative inferences. Such calculations are being planned and will be reported on in the future.

As far as we are aware, only outwardly propagating blobs have ever been observed in connection with the reconnection site underneath an erupting flux rope. Our simulation results, however, suggest the presence of comparable numbers of inwardly-propagating blobs. These blobs form at or below $2 R_{\odot}$ and thus would not be observable in the field of view of the *SOHO/LASCO C2* coronagraph ($2 R_{\odot} < r < 6 R_{\odot}$). However, they may be detectable in the future by coronagraphs onboard the *STEREO* spacecraft.

Work performed at SAIC was supported by the National Aeronautics and Space Administration (LWS and SECT Programs) and the National Science Foundation (The Center for Integrated Space Weather Modeling [CISM] and the SHINE Program).

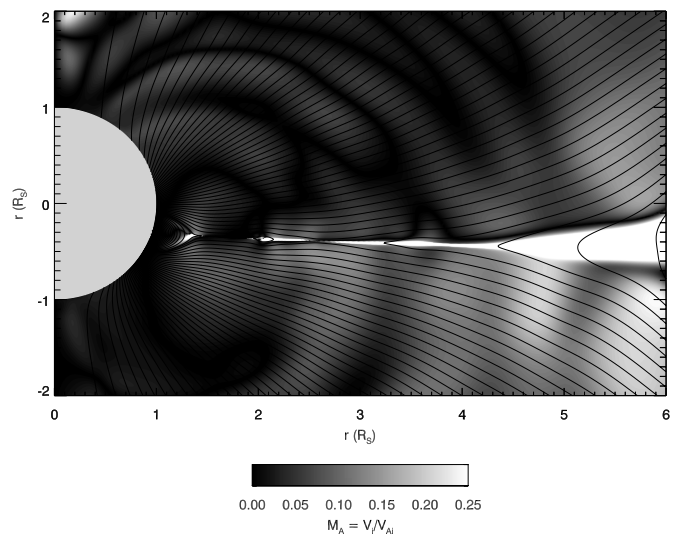


FIG. 6.—The Alfvén Mach number computed for $t = 42$ minutes following the first frame in Fig. 3 (i.e., between frames 2 and 3). Magnetic field lines are also shown. [See the electronic edition of the *Journal* for a color version of this figure.]

REFERENCES

- Antiochos, S. K., Devore, C. R., & Klimchuk, J. A. 1999, *ApJ*, 510, 485
- Bulanov, S. V., Syrovatskii, S. I., & Sakai, J. 1978, *J. Exp. Theor. Phys. Lett.*, 28, 177
- Dungey, J. W. 1953, *Phil. Mag.*, 44, 725
- Forbes, T. G. 2000, *J. Geophys. Res.*, 105, 23153
- Furth, H. P., Killeen, J., & Rosenbluth, M. N. 1963, *Phys. Fluids*, 6, 459
- Hiei, E., Hundhausen, A. J., & Sime, D. G. 1993, *Geophys. Res. Lett.*, 20, 2785
- Ko, Y.-K., Raymond, J. C., Lin, J., Lawrence, G., Li, J., & Fludra, A. 2003, *ApJ*, 594, 1068
- Lin, J., & Forbes, T. G. 2000, *J. Geophys. Res.*, 105, 2375
- Lin, J., Ko, Y.-K., Sui, L., Raymond, J. C., Stenborg, G. A., Jiang, Y., Zhao, S., & Mancuso, S. 2005, *ApJ*, 622, 1251
- Linker, J. A., & Mikić, Z. 1995, *ApJ*, 438, L45
- Linker, J. A., Mikić, Z., Lionello, R., Riley, P., Amari, T., & Odstrcil, D. 2003a, *Phys. Plasmas*, 10, 1971
- Linker, J. A., Mikić, Z., Riley, P., Lionello, R., & Odstrcil, D. 2003b, in *AIP Conf. Proc. 679, Solar Wind Ten*, ed. M. Velli, et al. (New York: AIP), 703
- Lionello, R., Mikić, Z., & Linker, J. A. 1998, *J. Comput. Phys.*, 140, 172
- McKenzie, D. E., & Hudson, H. S. 1999, *ApJ*, 519, L93
- . 2001, *Earth, Planets, Space*, 53, 577
- Mikić, Z., & Linker, J. A. 1994, *ApJ*, 430, 898
- Mikić, Z., Linker, J. A., Schnack, D. D., Lionello, R., & Tarditi, A. 1999, *Phys. Plasmas*, 6, 2217
- Priest, E., & Forbes, T. G. 2000, *Magnetic Reconnection: MHD Theory and Applications* (Cambridge: Cambridge Univ. Press)
- Riley, P., Linker, J. A., Mikić, Z., Odstrcil, D., Pizzo, V. J., & Webb, D. F. 2002, *ApJ*, 578, 972
- Riley, P., Linker, J. A., Mikić, Z., Odstrcil, D., Zurbuchen, T. H., Lario, D., & Lepping, R. P. 2003, *J. Geophys. Res. Space Phys.*, 108, 2
- Semenov, V. S., Heyn, M. F., & Kubyshkin, I. V. 1983, *Soviet Astron.*, 27, 660
- Sweet, P. A. 1958, *Nuovo Cimento Suppl.*, 8, 188
- Török, T., & Kliem, B. 2005, *ApJ*, 630, L97
- Tripathi, D., Bothmer, V., & Cremades, H. 2004, *A&A*, 422, 337
- Tripathi, D., Solanki, S. K., Schwenn, R., Bothmer, V., Mierla, M., & Stenborg, G. 2006, *A&A*, 449, 369
- Wang, Y.-M., Sheeley, N. R., Howard, R. A., St. Cyr, O. C., & Simnett, G. M. 1999, *Geophys. Res. Lett.*, 26, 1203
- Webb, D. F., Burkepile, J., Forbes, T. G., & Riley, P. 2003, *J. Geophys. Res.*, 108, 6